CHAPTER VIII
ELECTROSPINNING OF HEXANOYL CHITOSAN/POLYLACTIDE BLENDS

8.1 ABSTRACT

The electrospinning of hexanoyl chitosan (H-chitosan), polylactide (PLA), and their blends was performed using chloroform, dichloromethane, or tetrahydrofuran as a spinning solvent. The as-spun PLA fibers appeared to be round in their cross-section, with rough surface morphology, while the as-spun H-chitosan fibers were flat, with smooth surface morphology. The as-spun fibers from H-chitosan/PLA blend solutions in chloroform with the H-chitosan solution content of less than or equal to 50% w/w were continuous without the presence of beads, while those from the blend solutions in dichloromethane were beaded fibers or even just beads at high H-chitosan solution content. The diameters of the as-spun fibers from blend solutions with H-chitosan solution content of less than or equal to 50% w/w decreased with increasing amount of H-chitosan solution. Thermal characteristics and crystalline structure of selected as-spun fibers from pure and blend solutions in chloroform were characterized by thermo-gravimetric analysis (TGA), differential scanning calorimetry (DSC), and wide-angle X-ray diffraction (WAXD) techniques.

(**Key-words**: chitosan; hexanoyl chitosan; polylactide; polymer blend; electrospinning)

8.2 INTRODUCTION

Among the various aliphatic degradable polyesters, polylactide (PLA) has been considered as one of the most interesting and promising biodegradable materials and has been a material of choice to be used in various medical applications, such as surgical sutures [1], drug delivery vehicles [2], and bone fixtures [3]. The use of these products in vivo has a tremendous advantage over traditional ones due to the fact that PLA can be metabolized completely inside the body [4]. The increasing use of biodegradable polymers in medicine has attracted polymer scientists and the likes in pursuit of new materials that exhibit unique properties for specific uses in the field.

Chitosan or (1→4)-linked 2-amino-2-deoxy-β-*D*-glucan is a partially *N*-deacetylated derivative of chitin or poly(*N*-acetyl-*D*-glucosamine), one of the most abundant polysaccharides commonly found in shells of various insects and crustaceans as well as cell walls of various fungi. Chitosan has been explored as a suitable functional material for biomedical utilization, due mainly to its biocompatibility, biodegradability, and non-toxicity. Acylated chitosans, a series of chitosan derivatives, are soluble in various organic solvents, such as chloroform, benzene, pyridine, and tetrahydrofuran (THF). *N*-acylated chitosans have been fabricated as membranes [5], fibers [6], and films [7]. Among the various *N*-acylated chitosans, *N*-hexanoyl chitosan exhibited the best blood compatibility [8]. Furthermore, *N*-hexanoyl and *N*-octanoyl chitosans were found to be anti-thrombogenic and resistant to hydrolysis by lysozyme [9]. As a result, acylated chitosans are very attractive chitosan derivatives to be used in biomedical applications.

Polymer fibers are used in a wide variety of applications ranging from textiles to composite reinforcements. Traditional methods for obtaining polymer fibers include melt spinning [10], wet spinning, and gel spinning [11]. Recently, there has been increasing interest in another method of fiber production, i.e. electrostatic spinning or electrospinning, which can produce fibers that are sub-micrometers down to nanometers in diameter. The electrospinning process, first patented by Formhals

in 1934 [12], has been studied extensively particularly by Reneker and coworkers [13] and Vancso and coworkers [14] during the early re-visits of the technology. Via careful selections of the solution and the process parameters (e.g. solution concentration, applied electrostatic field strength, etc.), ultrafine fibers with diameters down to a few tens of nanometers could be fabricated.

In electrospinning a polymer solution, solvent is one of the main factor determining the spinnability of the solution. Water, a good solvent for poly(ethylene oxide) (PEO), was used in successful electrospinning of PEO [15-17]. When ethanol was added to water, the diameters of the resulting PEO fibers appeared to be larger and the beaded fibers earlier observed disappeared [15]. The reason was attributed to the reduction in the charge density carried by a charged jet and the increase in viscosity and evaporation rate of the resulting PEO solutions. Dimethylformamide (DMF) was used in successful electrospinning of polyacrylonitrile [18] and polyurethaneurea copolymer [19]; whereas, a mixed solvent of dichloromethane and DMF was required for successful electrospinning of poly(*p*-dioxanone-co-L-lactide)-b-poly(ethylene glycol) [20]. Solvents with high vapor pressures, e.g. carbondisulfide (CS_2), was thought to be the reason for the observed nanoporous morphology of electrospun polystyrene (PS) fibers and trichloromethane or chloromethane was found to be the best solvent for producing highly textured poly(methyl methacrylate) (PMMA) fibers [21].

Electrospun PLA fibers have been shown to have several applications for medical uses, such as wound dressing and tissue scaffolding [22-24]. Despite its potential applications in the medical area [8,9], successful electrospinning of hexanoyl chitosan (H-Chitosan) has not yet been reported in the open literature. Previously, we reported the characterization of H-chitosan/PLA blend films prepared by the solution-casting technique [25]. It was found that addition of H-chitosan helped improved the physical and mechanical of the normally brittle PLA film [25]. In the present contribution, electrospinning was applied to fabricate ultrafine fibers from pure H-chitosan, PLA, and their blends using chloroform, dichloromethane or tetrahydrofuran as the spinning solvent. Morphology and sizes of the as-spun fibers were investigated using scanning electron microscopy (SEM) and thermal behavior and crystalline structure of the as-spun fibers were investigated using thermo-

gravimetry analysis (TGA), differential scanning calorimetry (DSC), and wide-angle X-ray diffraction (WAXD).

8.3 EXPERIMENTAL

Materials

Chitosan having the degree of deacetylation of ca. 91% was prepared from Penaeus merguiensis shrimp shells by acid and alkali treatments. Chitosan was pulverized into powder, the size of which ranged from 71 to 75 μm, prior to further use. Hexanoyl chitosan (H-chitosan) was synthesized by reacting chitosan powder with hexanoyl chloride (Fluka, Switzerland) in a mixture of anhydrous pyridine (Sigma-Aldrich, USA) and chloroform (Sigma-Aldrich, USA) [26]. PLA was supplied as a courtesy from Daiseru Chemicals (Japan). The viscosity-average molecular weight ($\overline{M}_v$) of PLA was determined (based on viscosity measurements at 25°C in chloroform following the Mark-Houwink equation of the form [27]: $[\eta] = 7.4 \times 10^{-5} \cdot \overline{M}_v^{0.87}$) to be ca. 70,000 g·mol^{-1}. Chloroform, dichloromethane, or tetrahydrofuran, used as the spinning solvent, was purchased from Labscan (Asia) (Thailand).

Preparation of Electrospun Fibers

To prepare as-spun H-chitosan/PLA blends fibers, stock solutions of H-chitosan and PLA were first prepared separately using chloroform, dichloromethane, or tetrahydrofuran as the solvent. The concentration of H-chitosan stock solution was 10% w/v, while the concentration of PLA stock solutions was either 20 or 24% w/v. Slight stirring was used to expedite the dissolution and to homogenize the solutions. It should be noted that the 20% w/v PLA solution was prepared in order to illustrate the effect of the solution concentration on the resulting as-spun fibers. The stock solutions of H-chitosan/PLA blends were conveniently prepared by mixing the stock solutions of the pure material in the following weight ratios (H-chitosan/PLA): 80/20, 60/40, 50/50, 40/60, and 20/80, respectively).

To electrospin each of the stock solutions prepared, about 3 ml of the solution was filled in a 5-ml syringe, with a blunt-end, stainless steel needle (inner diameter = 0.9 mm) being attached at the opening end. Both the syringe and the needle was tilted 45° from a vertical line. The needle was connected to the emitting electrode of a Gamma High Voltage Research ES30P-5W high-voltage supply capable of generating a DC voltage in the range of 0 to 30 kV. An Al sheet, used as the collective screen, was connected to the ground electrode of the power supply and was placed perpendicular to the needle. The distance between the needle tip and the collective screen defines a collection distance. The applied electrostatic field strength was fixed at 16 kV/15 cm and the electrospinning process was carried out at room temperature (i.e. about 25°C) within a fixed collection time of 5 minutes.

Characterization

Shear viscosity of the H-chitosan/PLA blend solutions was measured using a Brookfield DV-III programmable viscometer at 25°C. Morphological appearance of the as-spun products was examined by a JEOL JSM-5200 scanning electron microscope (SEM). The specimens for SEM observation were prepared by cutting an Al sheet covered with the as-spun webs and the cut section was carefully affixed on a copper stub. Each sample was coated with thin layer of gold using a JEOL JFC-1100E ion sputtering device prior to observation under SEM. For each spinning condition, at least 80 measurements for the fiber diameters were recorded. Statistical analysis of the data obtained was carried out, from which an arithmetic mean and a standard deviation were reported.

Thermal properties of the as-spun products were analyzed by thermo-gravimetric analysis (TGA) and differential scanning calorimetry (DSC), respectively. TGA patterns were measured on a Perkin-Elmer Diamond TG/DTA analyzer at a heating rate of $10°C \cdot min^{-1}$ under nitrogen atmosphere over a scanning range of 50 to 500°C. Samples of about 5 to 10 mg were used. The melting characteristic and the crystalline structure of the as-spun products were analyzed by DSC and wide-angle X-ray diffraction (WAXD), respectively. DSC thermograms were recorded on a Mettler DSC 822e/400 analyzer at a heating rate of $10°C \cdot min^{-1}$

under nitrogen atmosphere, using the standard 40 μl pans (containing about 3 to 4 mg of samples). WAXD patterns were recorded on a Rigaku Rint2000 X-ray diffractometer. The X-ray source was Cu Kα. The scanning range and the scanning speed were 5 to 40° and 5 deg·s^{-1}, respectively.

8.4 RESULTS AND DISCUSSION

Morphology of As-spun Fibers

Chloroform, dichloromethane, or tetrahydrofuran was chosen as the solvent in this work because they were able to dissolve both H-chitosan and PLA into clear solutions. Some important properties of these solvents are summarized in Table 8.1. H-chitosan, PLA, and H-chitosan/PLA blend solutions were then prepared by physically mixing the stock solutions of H-chitosan and PLA in various weight ratios.

As-spun PLA Fibers

Chloroform and dichloromethane were able to dissolve PLA pellets to form a clear solution within 6 hours at room temperature, while tetrahydrofuran was able to do so within 1 hour at an elevated temperature (about 100°C). When the PLA solution in tetrahydrofuran was cooled down to room temperature, the formerly clear solution became increasingly viscous and cloudy. The viscosity and surface tension of the as-prepared PLA solutions in chloroform, dichloromethane and tetrahydrofuran were summarized in Table 8.2. Interestingly, the viscosity of the PLA solution in dichloromethane was the lowest (i.e. 178 cP), while that of the PLA solution in tetrahydrofuran was the highest (i.e. 778 cP). On the other hand, the surface tension of the PLA solution in tetrahydrofuran was the lowest (i.e. 28.5 mN·m^{-1}), while that of the PLA solution in dichloromethane was the highest (i.e. 44.5 mN·m^{-1}).

The morphological appearance of the as-spun fibers from 24% w/v PLA solutions in chloroform, dichloromethane, and tetrahydrofuran are shown in Figure 8.2. Obviously, the as-spun PLA fibers appeared to be circular in their cross-

section and the surface of the fibers appeared to be rough with pore-like structure being present. The fibers obtained from 24% w/v PLA solutions in chloroform and dichloromethane exhibited a bimodal diametric distribution (i.e. with the average diameters being 0.97 ± 0.33 and 4.63 ± 0.89 μm for fibers from 24% w/v PLA solution in chloroform and 0.86 ± 0.33 and 5.01 ± 1.30 μm for fibers from 24% w/v PLA solution in dichloromethane, respectively; see Table 8.3), while those obtained from 24% w/v PLA solution in tetrahydrofuran exhibited an average diameter of 2.17 ± 0.83 μm (see Table 8.3).

The pore-like structure on the surface of the fibers is postulated to be a result of the use of highly volatile solvents (see the boiling points listed in Table 8.1) and the microscopic phase separation of the solutions at the surface of the ejected, charged jet that occurred very rapidly during electrospinning. With the latter notion in mind, the solvent-rich phase readily transformed into the pore-like structure. With regards to the bimodal distribution of the fiber diameters, it could be explained that, during the flight of the ejected, charged jet from the needle to the collector plate, the primary jet could split apart into multiple, secondary jets, resulting in the formation of fibers of different diameters [28].

To investigate the effect of PLA concentration on diameters of the resulting PLA fibers, the as-spun fibers from 20% w/v PLA solution in dichloromethane were compared with those from the 24% w/v PLA solution. The diameters of the fibers obtained from the solution of greater concentration exhibited a much wider distribution, while the average values appeared to be quite comparable (see Table 8.3). Normally, the solution viscosity increased with increasing the solution concentration according to a power-law relationship [29] and an increase in the solution viscosity should result in the formation of fibers of larger diameters [30].

As-spun H-chitosan Fibers

Chloroform, dichloromethane, and tetrahydrofuran were able to dissolve H-chitosan to form a clear solution within 1 day. The viscosity and surface tension of the as-prepared H-chitosan solutions in chloroform, dichloromethane, and tetrahydrofuran were reported in Table 8.2. Interestingly, the viscosity values of the

H-chitosan solutions in chloroform and dichloromethane were much greater than those of the corresponding PLA solutions, while the surface tension values of the H-chitosan solutions in chloroform and dichloromethane were much lower than those of the corresponding PLA solutions. The viscosity of the H-chitosan solution in dichloromethane was the greatest (i.e. 2561 cP), while that of the H-chitosan solution in tetrahydrofuran was the lowest (i.e. 730 cP). On the other hand, the surface tension of the H-chitosan solution in dichloromethane was the greatest (i.e. 36.7 $mN \cdot m^{-1}$), while that of the H-chitosan solution in tetrahydrofuran was the lowest (i.e. 29.2 $mN \cdot m^{-1}$).

The morphological appearance of the as-spun fibers from 10% w/v H-chitosan solutions in chloroform, dichloromethane, and tetrahydrofuran are shown in Figure 8.3. Obviously, the as-spun H-chitosan fibers appeared to be ribbon-like, with smooth surface. Due to the fast evaporation of the solvents, the skin of the ejected, charged jet would "dry" first and once the skin dried out, further evaporation of the solvent from the core region caused the jet to collapse. During the process, the circular cross-section of the fibers became elliptical and finally flat. Even though such an explanation seemed reasonable to explain for formation of the flat fibers observed, but it was not able to explain why the cross-section of the as-spun PLA fibers appeared to be round, instead of being flat, since the solvents used were the same.

The average diameter of the as-spun fibers from 10% w/v H-chitosan solution in chloroform was 0.91 ± 0.40 μm, while that from 10% w/v H-chitosan solution in dichloromethane was 0.50 ± 0.19 μm (see Table 8.3). The greater dielectric constant of dichloromethane in comparison to that chloroform (see Table 8.1) could be one of the reasons for the observed smaller diameters of the obtained fibers, since greater dielectric constant leads to greater Coulombic repulsion force (responsible for the stretching of the charged jet and electrostatic force (responsible for the transport of the charged jet to the collective target) [31]. Another possible reason is the difference in the mass throughput of the solution from the needle. Due to the very low boiling point of dichloromethane, partial clogging of the needle could be the

reason for the much decrease in the mass throughput of the resulting solution from the needle, hence the much lower diameters of the fibers observed.

Contrarily to the electrospinning of the H-chitosan solutions in both chloroform and dichloromethane, the electrospinning of 10% w/v H-chitosan solution in tetrahydrofuran resulted in the much lower productivity (since the collection time was fixed at 5 minutes). Consequently, only chloroform and dichloromethane were chosen as the spinning solvent for further investigation.

As-spun H-chitosan/PLA Fibers

The viscosity of the as-prepared H-chitosan (10% w/v)/PLA (either 20 or 24% w/v) blend solutions in different blend compositions (in w/w) in chloroform and dichloromethane is listed in Table 8.4. Interestingly, the viscosity values of the blend solutions were found to decrease hypothetically with increasing amount of H-chitosan solution. The observed decrease in the viscosity with increasing amount of H-chitosan solution could be a result of the microscopic phase-separation.

Figures 8.4, 8.5 and 8.6 show SEM images of as-spun products from blend solutions of H-chitosan (10% w/v) and PLA (either 20 or 24% w/v) of varying weight ratio in chloroform and dichloromethane, respectively. Again, the applied electrostatic field strength was fixed at 16 kV/15 cm. Among the blend solutions in chloroform investigated, only the blend solutions containing 10% w/v H-chitosan solution not exceeding 50% w/w produced fibers with rough surface without the presence of beads (see Figure 8.4), while the blend solutions having greater amount of H-chitosan solution produced beaded fibers and beads with slight trace of ultrathin, smooth fibers, respectively. Interestingly, for as-spun fibers obtained from the blend solutions with H-chitosan solution content of less than or equal to 50% w/w, their diameters appeared to be a decreasing function of the amount of the H-chitosan solution added (see Table 8.3). This could be related to the observed decrease in the viscosity of the blend solutions (see Table 8.4), hence a decrease in the viscoelastic force in comparison with the Coulombic repulsion force [31]. Further decrease in the viscosity of the blend solutions (as the amount of H-chitosan increased further above 50% w/w) resulted in the formation of beaded fibers or just

beads, because the viscoelastic force in comparison with the Coulombic repulsion force was too low [31].

With regards to the blend solutions in dichloromethane investigated, the addition of H-chitosan solution into either 20 or 24% w/v PLA solutions decreased the viscosity of the blend solutions appreciably (see Table 8.4). Since the viscosity of these blend solutions even at the lowest H-chitosan solution content investigated (i.e. 20% w/w) was lower than that of the blend solution between 10% w/v H-chitosan and 24% w/v PLA solutions in chloroform that has the highest amount of H-chitosan investigated (i.e. 80% w/w), it is expected that the blend solutions in dichloromethane should only produce beaded fibers or just beads. Indeed, beaded fibers were observed even at the lowest H-chitosan solution content investigated (i.e. 20% w/w) (see Figures 8.5a and 8.6a). Apparently, the diameters of the beaded fibers decreased with further increase in the H-chitosan solution content (see Table 8.3), while the number of beads per unit area increased with increasing amount of H-chitosan solution in the blend solutions (see Figures 8.5 and 8.6). As expected, the observed decrease in the diameters of the beaded fibers with increasing H-chitosan solution content was a result of the decrease in the viscosity, hence the decrease in the viscoelastic force in comparison with the Coulombic repulsion force [31], of the resulting blend solutions.

Characterization of As-spun H-chitosan/PLA Fibers

Since only H-chitosan/PLA blend solutions containing H-chitosan solution content of up to 40% w/w in chloroform could be electrospun into continuous fibers without the presence of beads, only the fibers obtained from these blend solutions were further characterized in comparison with the fibers obtained from pure solutions of H-chitosan and PLA.

Thermal Properties

Thermal stability of the as-spun H-chitosan, PLA, and corresponding H-chitosan/PLA fibers (from blend solutions containing H-chitosan solution of 20 and 40% w/w) was evaluated by TGA technique. Figure 8.7 shows TGA thermograms of these as-spun fibers. According to the derivative TGA curves, pure

as-spun PLA fibers were found to degrade at ca. 340°C, while pure as-spun H-chitosan fibers exhibited two degradation peaks at ca. 253 and 322°C, respectively. Previously, we reported that pure PLA film degraded at ca. 327°C, while pure H-chitosan film showed two degradation peaks at ca. 257 and 327°C, respectively [25]. Evidently, thermal stability of the as-spun fibers and the as-cast films of pure H-chitosan and PLA were very close. As for H-chitosan/PLA fibers, the fibers from blend solutions containing 20 or 40% w/w H-chitosan solution exhibited only one degradation peak at ca. 326 and 336°C, respectively.

Figure 8.8 illustrates the 2nd heating thermograms of the as-spun H-chitosan, PLA, and corresponding H-chitosan/PLA fibers. Evidently, no thermal transition of any kind was discernable in the heating thermogram of pure as-spun H-chitosan fibers. For both pure as-spun PLA and corresponding H-chitosan/PLA fibers, two melting endotherms were visualized. Based on related studies on the multiple-melting behavior of some semi-crystalline polymers [32,33], the occurrence of the low-temperature melting endotherm (T_{ml}) was usually attributed to the melting of the primary crystals formed during the primary cooling, while that of the high-temperature melting endotherm (T_{mh}) was to the melting of the re-crystallized crystals formed during the subsequent heating scan.

Apparently, the T_{ml} and the T_{mh} values for all of the pure as-spun PLA and corresponding H-chitosan/PLA fibers investigated are located at ca. 162 and 170°C, respectively. These values are comparable to the values reported in an earlier report [25]. Qualitatively, the area under the melting endotherm related directly to the amount of the crystals present within the samples. Since the high-temperature melting endotherm related to the melting of the re-crystallized crystals, only the low-temperature melting one should only be accounted for the amount of the crystals present within each sample. According to Figure 8.8, the fractional area of the low-temperature melting endotherm for samples electrospun from solutions of each respective blend ratio decreased monotonically with increasing H-chitosan solution content. Specifically, the ΔH_f value decreased monotonically from ca. 27.4 $J \cdot g^{-1}$ for pure as-spun PLA fibers to ca. 21.4 and to 18.7 $J \cdot g^{-1}$ for as-spun H-chitosan/PLA

fibers from blend solution containing 20 and 40% w/w H-chitosan solutions, respectively.

Crystalline Structure

WAXD patterns of the as-spun H-chitosan, PLA, and corresponding H-chitosan/PLA fibers are illustrated in Figure 8.9. Obviously, the WAXD pattern of pure as-spun H-chitosan fibers exhibited a sharp diffraction peak at the scattering angle 2θ of ca. 5.8° along with a broad diffraction peak centering at the 2θ of ca. 20.0°, which are in excellent agreement with the values obtained previously for as-cast H-chitosan film [25]. The sharp diffraction peak at about 5.8° was reported to be a result of the interdegitation of the hexanoyl side-chains with the extended main chains forming a layer structure, while the broad diffraction peak at about 20.0° was a result of the loss of crystallinity due to the loss of hydrogen bonding [26]. Interestingly, the interdegitation of the hexanoyl side-chains was not lost when H-chitosan was fabricated into ultrafine fibers using the electrospinning technique.

For pure as-spun PLA fibers, the obtained WAXD pattern showed only one broad diffraction peak centering at the 2θ of ca. 17.5°, which is in good agreement with the value earlier reported for as-cast PLA film [25]. When crystallizing in a pseudo-orthorhombic unit cell (with axes a = 1.07 nm, b = 0.595 nm, and c = 2.78 nm), PLA should show main diffraction peaks at the 2θ's of 15, 17, and 19° [34]. For as-spun H-chitosan/PLA fibers, the obtained diffraction patterns apparently exhibited only one broad diffraction peak centering at about the same 2θ value as that of pure as-spun PLA fibers. No indication of the characteristic peak at low diffraction angles was observed, suggesting that the actual content of H-chitosan in the as-spun H-chitosan/PLA fibers was very low, since it was reported earlier that as-cast H-chitosan/PLA film having H-chitosan content of as low as 20% w/w exhibited the characteristic peak at low diffraction angles (due to the layer structure of the main chains of H-chitosan upon the interdegitation of the hexanoyl side-chains [26]).

8.5 CONCLUSIONS

Electrospun hexanoyl chitosan (H-chitosan), polylactide (PLA), and H-chitosan/PLA fibers were prepared from solutions of H-chitosan/PLA in chloroform, dichloromethane, and tetrahydrofuran. The as-spun fibers from PLA solutions in all of the three solvents appeared to be round in their cross-section, with rough surface morphology, while the as-spun fibers from H-chitosan solutions in all of the three solvents were flat, with smooth surface morphology. The electrospinning of H-chitosan solution in tetrahydrofuran did not produce the as-spun fibers with high enough productivity. The as-spun fibers from H-chitosan/PLA blend solutions in chloroform with the H-chitosan solution content of less than or equal to 50% w/w were continuous without the presence of beads, while those from the blend solutions in dichloromethane were beaded fibers or even just beads at high H-chitosan solution content. Interestingly, the diameters of the as-spun fibers from blend solutions with H-chitosan solution content of less than or equal to 50% w/w were found to decrease with increasing amount of H-chitosan solution. The most likely explanation was due to the observed decrease in the solution viscosity with increasing amount of H-chitosan solution. With regards to thermal stability of the as-spun fibers, both as-spun PLA and H-chitosan/PLA fibers exhibited one degradation peak, while as-spun H-chitosan fibers exhibited two degradation peaks. The second heating thermogram of as-spun PLA and H-chitosan/PLA fibers exhibited multiple melting phenomenon, while that of as-spun H-chitosan fibers did not show any sign of the thermal transition. Lastly, wide-angle X-ray diffraction showed that as-spun H-chitosan fibers exhibited a sharp diffraction peak at ca. 5.8° and a broad diffraction peak centering at ca. 20°, while both as-spun PLA and H-chitosan/PLA fibers showed a broad diffraction peak centering at ca. 17.5°.

8.6 ACKNOWLEDGMENTS

The authors acknowledge partial supports received from the National Research Council of Thailand (under a research program "Nanopolymer"), the

Petroleum and Petrochemical Technology Consortium [through a Thai governmental loan from the Asian Development Bank (ADB)], and the Petroleum and Petrochemical College (PPC), Chulalongkorn University.

8.7 REFERENCES

[1] L. Fambri, A. Pegoretti, R. Fenner, S.D. Incardona and C. Migliaresi, *Polymer* 38, 79 (1997).

[2] G. Khang, J.M. Rhee, J.K. Jeong, J.S. Lee, M.S. Kim, S.H. Cho and H.B. Lee, *Macromolecular Research* 11, 207 (2003).

[3] J.E. Bergsma, R.R.M. Bos, F.R. Rozema, W.D. Jong and G. Boering, *Journal of Materials Science – Materials In Medicine* 7, 1 (1996).

[4] J.E. Bergsma, F.R. Rozema, R.R.M. Bos, G. Boering, W.C. Brujin and A.J. Pennings, *Biomaterials* 16, 267 (1995).

[5] Y. Seo, H. Ohtake, T. Unishi and T. Iijima, *Journal of Applied Polymer Science* 58, 633 (1995).

[6] S. Hirano, A. Usutani, M. Yoshikawa and T. Midorikawa, *Carbohydrate Polymers* 37, 311 (1998).

[7] D. Xu, S.P. McCarthy, R.A. Gross and D.L. Kaplan, *Macromolecules* 29, 3436 (1996).

[8] K.Y. Lee, W.S. Ha and W.H. Park, *Biomaterials* 16, 1211 (1995).

[9] S. Hirano and Y. Noishiki, *Journal of Biomedical Materials Research* 19, 413 (1985).

[10] J.R. Dees and J.E. Spruiell, *Journal of Applied Polymer Science* 18, 1053 (1974).

[11] P.J. Barham and A. Keller, *Journal of Materials Science* 20, 2281 (1985).

[12] A. Formhals, US Patent 1 975 504 (1934).

[13] D.H. Reneker, A.L. Yarin, H. Fong and S. Koombhonge, *Journal of Applied Physics* 87, 4531 (2000).

[14] R. Jaeger, M.M. Bergshoef, I. Martin, C. Battle, H. Schonherr and G.J. Vancso, *Macromolecular Symposia* 127, 141 (1998).

[15] H. Fong, I. Chun and D.H. Reneker, *Polymer* 40, 4585 (1999).

[16] R. Jaeger, H. Schonherr and G.J. Vancso, *Macromolecules* 29, 7634 (1996).

[17] Y.M. Shin, M.M. Hohman, M.P. Brenner and G.C. Rutledge, *Polymer* 42, 9955 (2001).

[18] C.J. Buchko, J.C. Chen, Y. Shen and D.C. Martin, *Polymer* 40, 7397 (1999).

[19] M.M. Demir, I. Yilgor, E. Yilgor and B. Erman, *Polymer* 43, 3303 (2002).

[20] S.R. Bhattarai, N. Bhattarai, H.K. Yi, P.H. Hwang, D.I. Cha and H.Y. Kim, *Biomaterials* 25, 2595 (2004).

[21] S. Megelski, J.S. Stephens, D.B. Chase and J.F. Rabolt, *Macromolecules* 35, 8456 (2002).

[22] F. Yang, R. Murugan, S. Wang and S. Ramakrishna, *Biomaterials* 26, 2603 (2005).

[23] M. Bognitzki, W. Czado, T. Frese, A. Schaper, M. Hellwig, M. Steinhart, A. Greinier and J. Wendorff, *Advanced Materials* 13, 70 (2001).

[24] J. Zeng, X. Chen, X. Xu, Q. Liang, X. Bian, L. Yang and X. Jing, *Journal of Applied Polymer Science* 89, 1085 (2003).

[25] M. Peesan, P. Supaphol and R. Rujiravanit, *Carbohydrate Polymers*, in press.

[26] Z. Zong, Y. Kimura, M. Takahashi and H. Yamane, *Polymer* 41, 899 (2000).

[27] G. Rafler, J. Dahlmann and K. Wiener, *Acta Polymerica* 41, 328 (1990).

[28] S. Koombhongse, W.X. Liu and D.H. Reneker, *Journal of Polymer Science – B: Polymer Physics* 39, 2598 (2001).

[29] J.M. Deitzel, J. Kleinmeyer, K. Harris and N.C. Beck Tan, *Polymer* 42, 261 (2001).

[30] J. Doshi and D.H. Reneker, *Journal of Electrostatics* 35, 151 (1995).

[31] L. Wannatong, A. Sirivat and P. Supaphol, *Polymer International* 53, 1851 (2004).

[32] P. Supaphol, *Journal of Applied Polymer Science* 82, 1083 (2001).

[33] P. Srimoaon, N. Dangseeyun and P. Supaphol, *European Polymer Journal* 40, 599 (2004).

[34] G. Kister, G. Cassanas and M. Vert, *Polymer* 39, 267 (1998).

8.8 CAPTION OF FIGURES

Figure 8.1 Chemical structure of perfectly substituted H-chitosan.

Figure 8.2 SEM images (magnification = 2000x and scale bar = 10 μm) of as-spun fibers from 24% w/v PLA solutions in (a) chloroform, (b) dichloromethane, and (c) tetrahydrofuran. The applied electrostatic field strength was 16 kV/15 cm.

Figure 8.3 SEM images (magnification = 2000x and scale bar = 10 μm) of as-spun fibers from 10% w/v H-chitosan solutions in (a) chloroform, (b) dichloromethane, and (c) tetrahydrofuran. The applied electrostatic field strength was 16 kV/15 cm.

Figure 8.4 SEM images (magnification = 500x and scale bar = 50 μm) of as-spun products from blend solutions of H-chitosan (10% w/v in chloroform) and PLA (24% w/v in chloroform) in various blend compositions (w/w): (a) 20/80, (b) 40/60, (c) 50/50, (d) 60/40, and (e) 80/20, respectively. The applied electrostatic field strength was 16 kV/15 cm.

Figure 8.5 SEM images (magnification = 500x and scale bar = 50 μm) of as-spun products from blend solutions of H-chitosan (10% w/v in dichloromethane) and PLA (20% w/v in dichloromethane) in various blend compositions (w/w): (a) 20/80, (b) 40/60, (c) 50/50, (d) 60/40, and (e) 80/20, respectively. The applied electrostatic field strength was 16 kV/15 cm.

Figure 8.6 SEM images (magnification = 500x and scale bar = 50 μm) of as-spun products from blend solutions of H-chitosan (10% w/v in dichloromethane) and PLA (24% w/v in dichloromethane) in various blend compositions (w/w): (a) 20/80, (b) 40/60, (c) 50/50, (d) 60/40, and (e) 80/20, respectively. The applied electrostatic field strength was 16 kV/15 cm.

Figure 8.7 TGA thermograms of as-spun H-chitosan, PLA, and H-chitosan/PLA fibers. The fibers were spun from pure or blend solutions in chloroform and the heating rate used was $10°C \cdot min^{-1}$.

Figure 8.8 Second heating thermograms of as-spun H-chitosan, PLA, and H-chitosan/PLA fibers. The fibers were spun from pure or blend solutions in chloroform and the heating rate used was $10°C \cdot min^{-1}$.

Figure 8.9 WAXD patterns of as-spun H-chitosan, PLA, and H-chitosan/PLA fibers. The fibers were spun from pure or blend solutions in chloroform.

Table 8.1 Some important properties of solvents used

Solvent	Boiling point (°C)	Solubility parameter $(Cal \cdot cm^{-3})^{1/2}$	Surface tension $(mN \cdot m^{-1})$	Density $(g \cdot cm^{-3})$	Dipole moment (debye)	Dielectric constant	Viscosity (cP)
Chloroform	61.2	9.34	26.0	1.470	1.15	4.81	0.58
Dichloromethane	40.0	9.70	28.6	1.327	1.55	9.10	0.44
Tetrahydrofuran	66.0	9.10	24.4	0.875	1.75	7.60	0.55

Table 8.2 Viscosity and surface tension of 10% w/v H-chitosan and 24% w/v PLA solutions in chloroform, dichloromethane, and tetrahydrofuran

Solvent	Viscosity (cP)		Surface tension ($mN \cdot m^{-1}$)	
	H-chitosan	PLA	H-chitosan	PLA
Chloroform	1067	418	34.9	40.3
Dichloromethane	2561	178	36.7	44.5
Tetrahydrofuran	730	778	29.2	28.5

Table 8.3 Observed average diameter of as-spun fibers from pure and blend solutions of H-chitosan (10% w/v in chloroform and dichloromethane) and PLA (24% w/v in chloroform and 20 or 24% w/v in dichloromethane). The applied electrostatic field strength was 16kv/15 cm

H-chitosan/PLA blend composition (w/w)	Average fiber diameter (μm)					
	10% w/v H-chitosan and 24% w/v PLA solutions in chloroform		10% w/v H-chitosan and 20% w/v PLA solutions in dichloromethane		10% w/v H-chitosan and 24% w/v PLA solutions in dichloromethane	
100/0	0.91 ± 0.40		-		0.50 ± 0.19	
80/20	0.20 ± 0.08	-	n/a*	-	n/a*	-
60/40	0.28 ± 0.21	-	0.70 ± 0.24	-	0.74 ± 0.28	-
50/50	0.48 ± 0.37	3.17 ± 0.99	0.98 ± 0.35	2.65 ± 0.31	0.92 ± 0.37	2.30 ± 0.83
40/60	0.80 ± 0.55	3.25 ± 1.11	1.19 ± 0.37	3.57 ± 1.23	1.21 ± 0.35	2.38 ± 0.24
20/80	1.26 ± 0.46	3.77 ± 1.20	1.26 ± 0.46	3.60 ± 1.19	1.26 ± 0.42	4.07 ± 1.67
0/100	0.97 ± 0.33	4.63 ± 0.89	1.30 ± 0.45	4.59 ± 2.24	0.86 ± 0.34	5.01 ± 1.30

*Only beads were observed

Table 8.4 Apparent shear viscosity of pure and blend solutions of H-chitosan (10% w/v in chloroform and dichloromethane) and PLA (24% w/v in chloroform and 20 or 24% w/v in dichloromethane)

H-chitosan/PLA blend composition (w/w)	Viscosity (cP)		
	10% w/v H-chitosan and 24% w/v PLA solutions in chloroform	10% w/v H-chitosan and 20% w/v PLA solutions in dichloromethane	10% w/v H-chitosan and 24% w/v PLA solutions in dichloromethane
100/0	1067.0	2561.0	2561.0
80/20	156.0	44.0	34.5
60/40	138.0	31.0	68.5
50/50	151.0	41.0	63.0
40/60	220.0	77.4	75.0
20/80	770.0	96.6	121.0
0/100	418.0	154.0	178.0

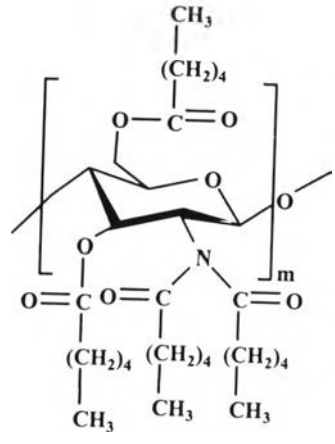

Figure 8.1

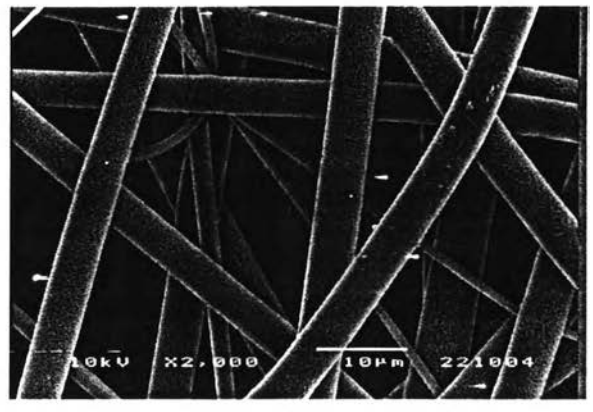

(a)

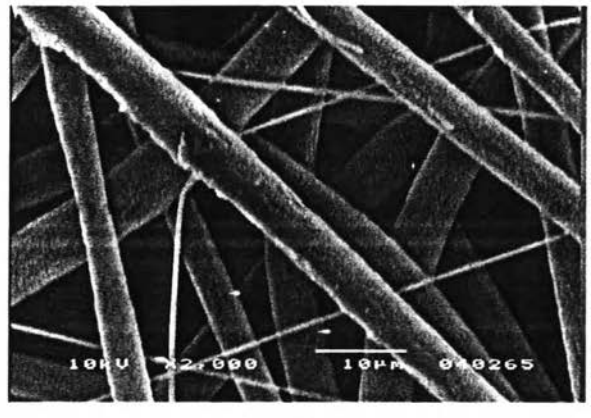

(b)

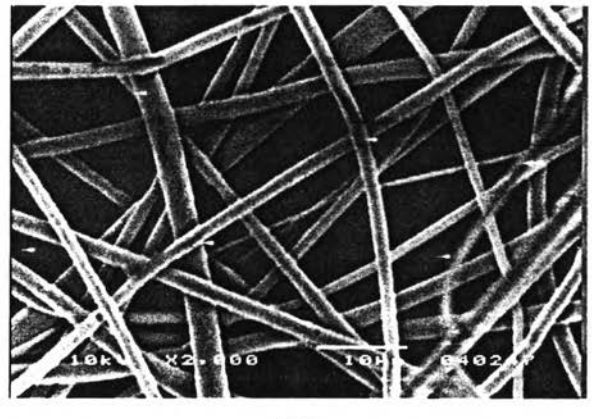

(c)

Figure 8.2

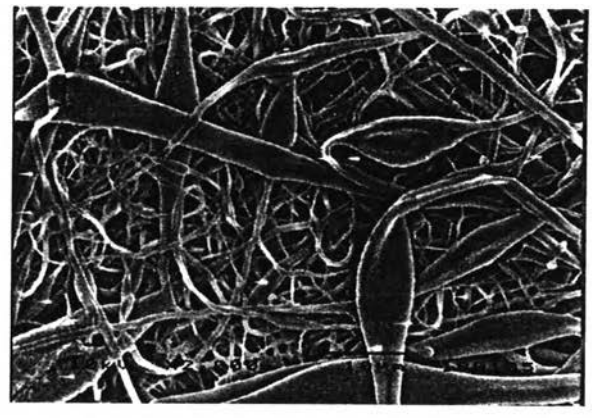

(a)

(b)

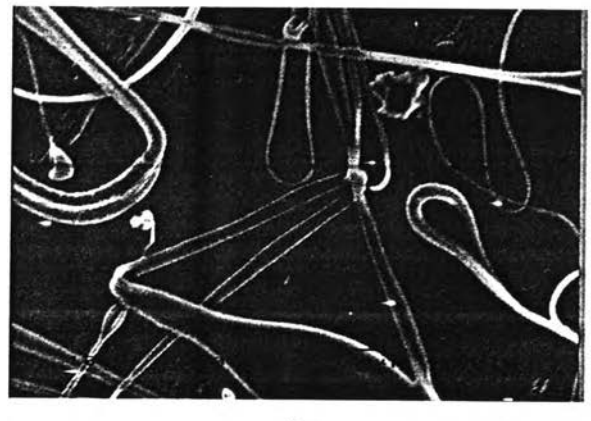

(c)

Figure 8.3

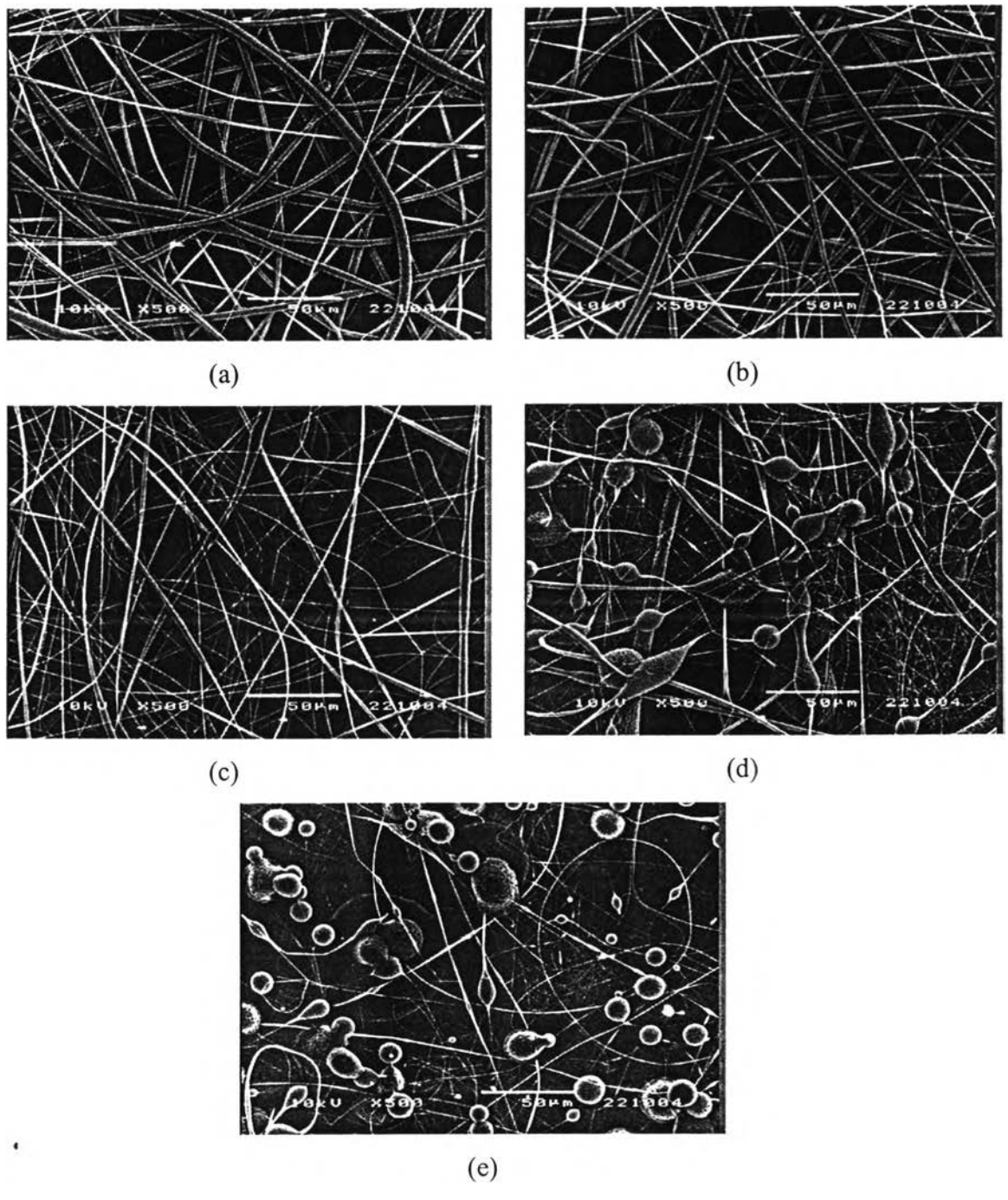

Figure 8.4

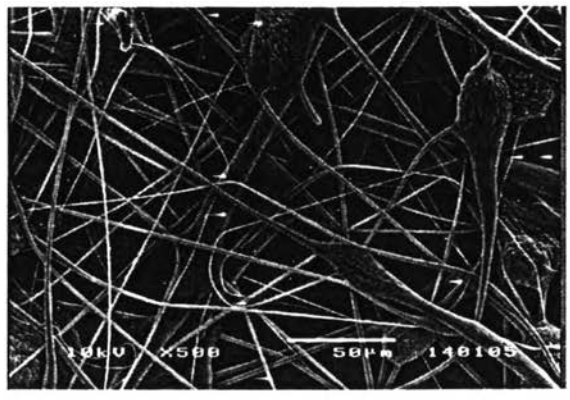

(a)

(c)

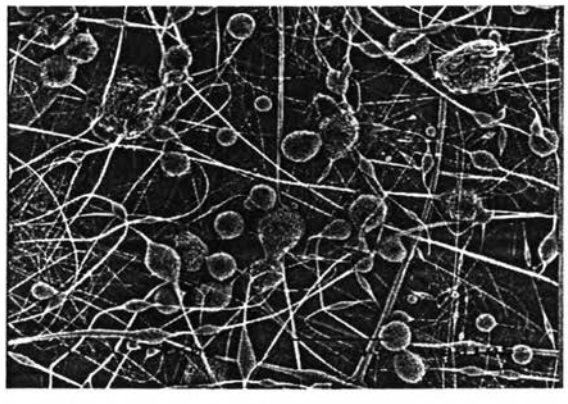

(b)

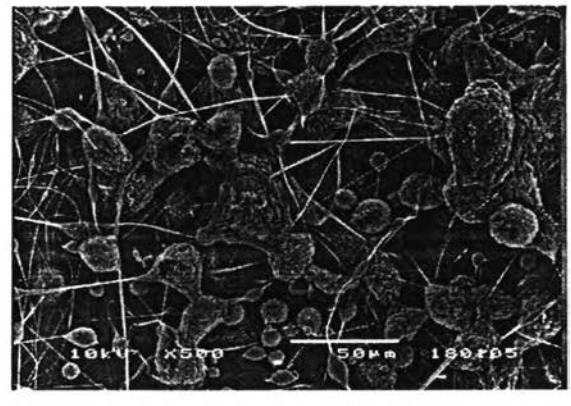

(d)

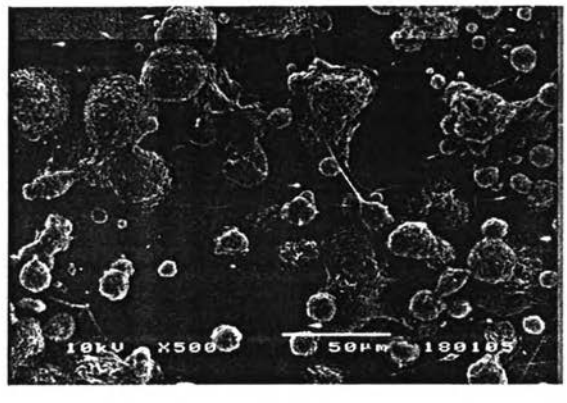

(e)

Figure 8.5

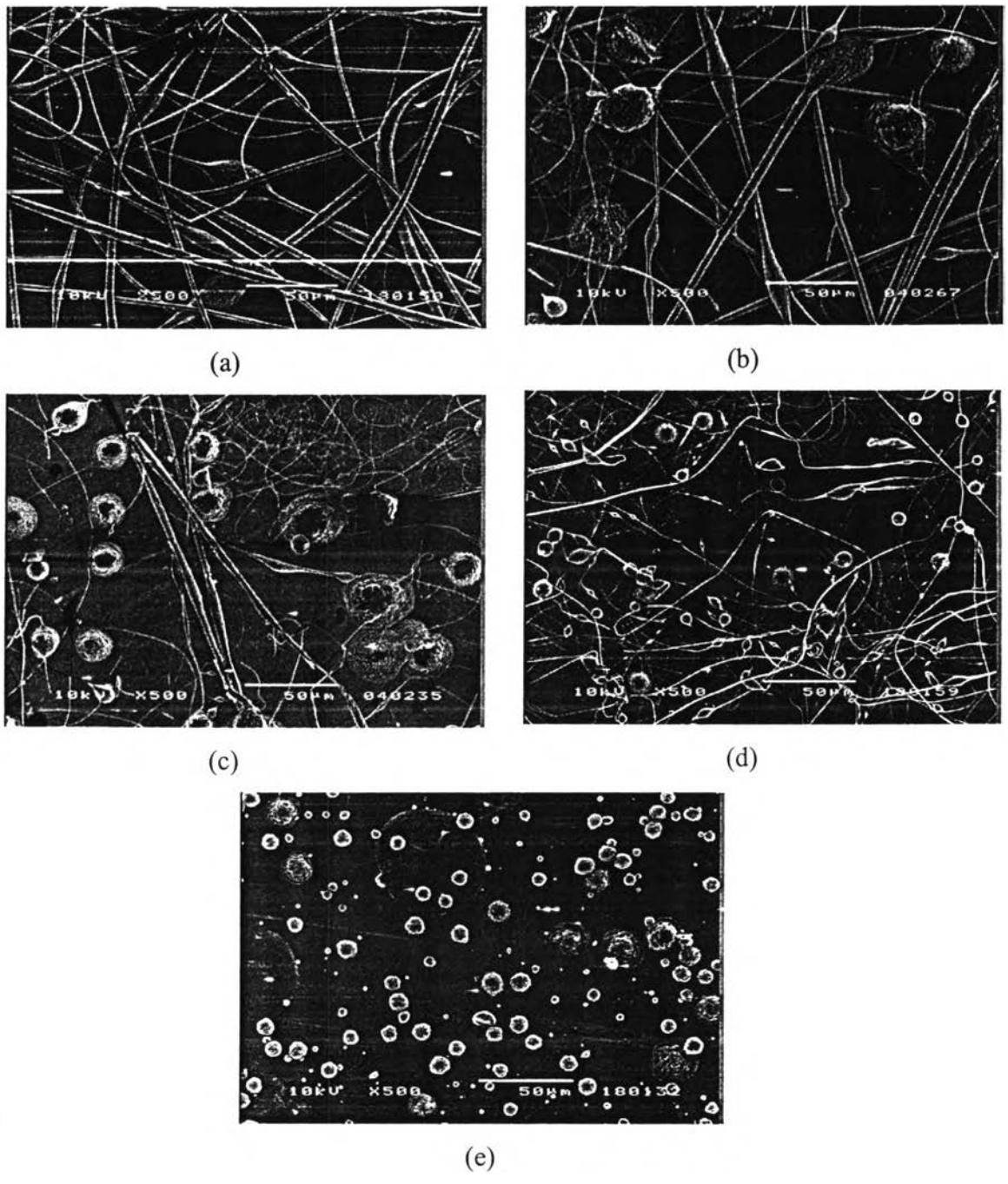

Figure 8.6

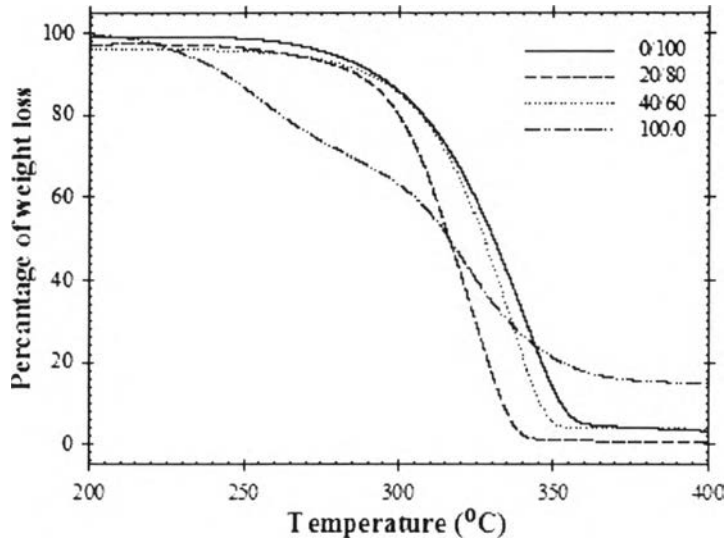
Percentage of weight loss
Temperature (°C)
0:100
20:80
40:60
100:0
100
80
60
40
20
0
200
250
300
350
400

Figure 8.7

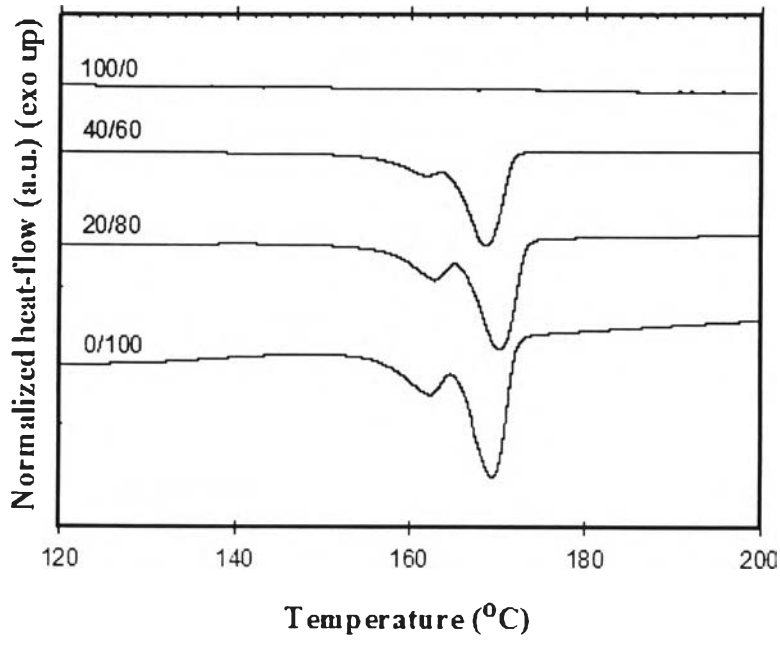
Normalized heat-flow (a.u.) (exo up)
100/0
40/60
20/80
0/100
120
140
160
180
200
Temperature (°C)

Figure 8.8

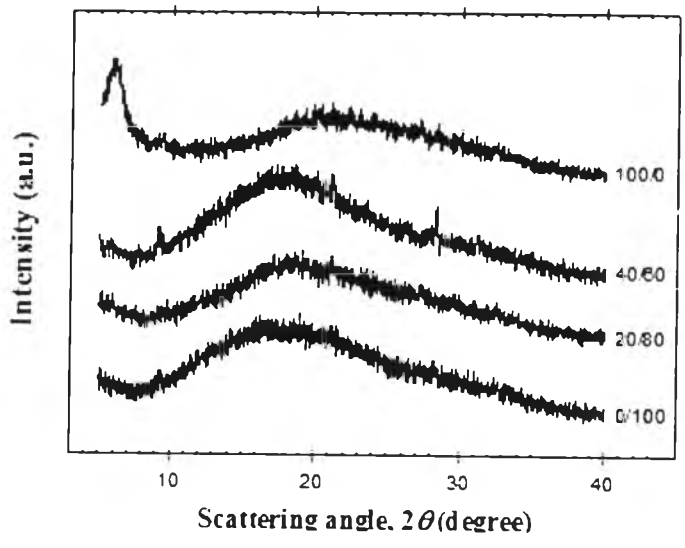
Intensity (a.u.)
100/0
40/60
20/80
0/100
10
20
30
40
Scattering angle, 2θ (degree)

Figure 8.9